



Article

Aprotinin Inhibits SARS-CoV-2 Replication

Denisa Bojkova ¹, Marco Bechtel ¹, Katie-May McLaughlin ², Jake E. McGreig ² , Kevin Klann ³ , Carla Bellinghausen ⁴ , Gernot Rohde ⁴ , Danny Jonigk ^{5,6}, Peter Braubach ^{5,6}, Sandra Ciesek ^{1,7,8} , Christian Münch ^{3,9,10} , Mark N. Wass ^{2,*} , Martin Michaelis ^{2,*}  and Jindrich Cinatl, Jr. ^{1,*}

¹ Institute for Medical Virology, University Hospital, Goethe University, 60596 Frankfurt am Main, Germany; Denisa.Bojkova@kgu.de (D.B.); marco.bechtel@kgu.de (M.B.); Sandra.ciesek@kgu.de (S.C.)

² School of Biosciences, University of Kent, Canterbury CT2 7NJ, UK; km625@kent.ac.uk (K.-M.M.); jem53@kent.ac.uk (J.E.M.)

³ Faculty of Medicine, Institute of Biochemistry II, Goethe University, 60590 Frankfurt am Main, Germany; klann@em.uni-frankfurt.de (K.K.); ch.muench@em.uni-frankfurt.de (C.M.)

⁴ Department of Respiratory Medicine and Allergology, University Hospital, Goethe University, 60590 Frankfurt am Main, Germany; c.bellinghausen@med.uni-frankfurt.de (C.B.); Gernot.rohde@kgu.de (G.R.)

⁵ Institute of Pathology, Hannover Medical School (MHH), 30625 Hannover, Germany; jonigk.danny@mh-hannover.de (D.J.); Braubach.Peter@mh-hannover.de (P.B.)

⁶ Biomedical Research in Endstage and Obstructive Lung Disease Hannover (BREATH), The German Center for Lung Research (Deutsches Zentrum für Lungenforschung, DZL), Hannover Medical School (MHH), 30625 Hannover, Germany

⁷ German Center for Infection Research, DZIF, External Partner Site, 60596 Frankfurt am Main, Germany

⁸ Fraunhofer Institute for Molecular Biology and Applied Ecology (IME), Branch Translational Medicine und Pharmacology, 60596 Frankfurt am Main, Germany

⁹ Frankfurt Cancer Institute, Goethe University, 60596 Frankfurt am Main, Germany

¹⁰ Cardio-Pulmonary Institute, Goethe University, 60590 Frankfurt am Main, Germany

* Correspondence: M.N.Wass@kent.ac.uk (M.N.W.); M.Michaelis@kent.ac.uk (M.M.); Cinatl@em.uni-frankfurt.de (J.C.J.)

Received: 28 June 2020; Accepted: 28 October 2020; Published: 30 October 2020



Abstract: Severe acute respiratory syndrome virus 2 (SARS-CoV-2) is the cause of the current coronavirus disease 19 (COVID-19) pandemic. Protease inhibitors are under consideration as virus entry inhibitors that prevent the cleavage of the coronavirus spike (S) protein by cellular proteases. Herein, we showed that the protease inhibitor aprotinin (but not the protease inhibitor SERPINA1/alpha-1 antitrypsin) inhibited SARS-CoV-2 replication in therapeutically achievable concentrations. An analysis of proteomics and transcriptome data indicated that SARS-CoV-2 replication is associated with a downregulation of host cell protease inhibitors. Hence, aprotinin may compensate for downregulated host cell proteases during later virus replication cycles. Aprotinin displayed anti-SARS-CoV-2 activity in different cell types (Caco2, Calu-3, and primary bronchial epithelial cell air–liquid interface cultures) and against four virus isolates. In conclusion, therapeutic aprotinin concentrations exert anti-SARS-CoV-2 activity. An approved aprotinin aerosol may have potential for the early local control of SARS-CoV-2 replication and the prevention of COVID-19 progression to a severe, systemic disease.

Keywords: severe acute respiratory syndrome coronavirus; severe acute respiratory syndrome coronavirus 2; 2019-nCoV; COVID-19; antiviral; drug discovery; aprotinin

1. Introduction

Severe acute respiratory syndrome virus 2 (SARS-CoV-2), a novel betacoronavirus, causes a respiratory disease and pneumonia called coronavirus disease 19 (COVID-19) and is the cause of a current pandemic responsible for millions of cases and hundreds of thousands of deaths [1–7]. Drugs for the treatment of COVID-19 are urgently needed.

Cell entry of coronaviruses is mediated by the interaction of the viral spike (S) protein with their host cell receptors, which differ between different coronaviruses [8]. For example, Middle East respiratory syndrome coronavirus (MERS-CoV) uses dipeptidyl peptidase 4 (DPP4) as a cellular receptor [8]. Host cell entry of SARS-CoV-2 and of the closely related severe acute respiratory syndrome virus (SARS-CoV) is mediated by angiotensin-converting enzyme 2 (ACE2) [8–10]. S binding to ACE2 depends on S cleavage at three sites (S1, S2, and S2') by host cell proteases, typically by the transmembrane serine protease 2 (TMPRSS2), and can be inhibited by serine protease inhibitors [9,10]. Camostat was the first serine protease inhibitor that was shown to inhibit TMPRSS2 [9]. Subsequently, additional TMPRSS2 inhibitors, including nafamostat and Arbidol derivatives, were demonstrated to interfere with SARS-CoV-2 internalization into host cells [11–13].

Aprotinin is a serine protease inhibitor, which has previously been shown to inhibit TMPRSS2 and has been suggested as a treatment option for influenza viruses and coronaviruses [14,15]. Herein, we investigated the effects of aprotinin against SARS-CoV-2.

2. Materials and Methods

2.1. Drugs

SERPINA1/alpha-1 antitrypsin (Prolastin) was obtained from Grifols (Barcelona, Spain). Aprotinin was purchased from Sigma-Aldrich (Darmstadt, Germany).

2.2. Cell Culture

The Caco2 cell line was obtained from DSMZ (Braunschweig, Germany), and Calu-3 from ATCC (Manassas, VA, US). The cells were grown at 37 °C in minimal essential medium (MEM) supplemented with 10% fetal bovine serum (FBS), 100 IU/mL of penicillin, and 100 µg/mL of streptomycin. All culture reagents were purchased from Sigma-Aldrich. Cells were regularly authenticated by short tandem repeat (STR) analysis and tested for mycoplasma contamination.

Lung tissue for the isolation of primary epithelial cells was provided by the Hannover Medical School, Institute of Pathology (Hannover, Germany). The use of tissue was approved by the ethics committee of the Hannover Medical School (MHH, Hannover, Germany, number 2701–2015) and was in compliance with The Code of Ethics of the World Medical Association. Primary bronchial epithelial cells were isolated from the lung explant tissue of a patient with lung emphysema as described previously [16]. All patients or their next of kin gave written informed consent for the use of their lung tissue for research. Basal cells were expanded in Keratinocyte-SFM medium supplemented with bovine pituitary extract (25 µg/mL), human recombinant epidermal growth factor (0.2 ng/mL, all from Gibco, Schwerte, Germany), isoproterenol (1 nM, Sigma), Antibiotic/Antimycotic Solution (Sigma-Aldrich), and MycoZap Plus PR (Lonza, Cologne, Germany) and cryopreserved until further use.

For differentiation, the cells were thawed and passaged once in PneumaCult-Ex Medium (StemCell Technologies, Cologne, Germany) and then seeded on transwell inserts (12-well plate, Sarstedt, Nümbrecht, Germany) at 4×10^4 cells/insert. Once the cell layers reached confluency, the medium on the apical side of the transwell was removed, and medium in the basal chamber was replaced with PneumaCult ALI Maintenance Medium (StemCell Technologies), including Antibiotic/Antimycotic Solution (Sigma-Aldrich) and MycoZap Plus PR (Lonza). During a period of four weeks, the medium was changed and the cell layers were washed with PBS every other day. Criteria for successful differentiation were the development of ciliated cells and ciliary movement, an increase in transepithelial electric resistance indicative of the formation of tight junctions, and mucus production.

2.3. Virus Infection

The isolates SARS-CoV-2/1/Human/2020/Frankfurt (SARS-CoV-2/FFM1), SARS-CoV-2/2/Human/2020/Frankfurt (SARS-CoV-2/FFM2), SARS-CoV-2/6/Human/2020/Frankfurt (SARS-CoV-2/FFM6), and SARS-CoV-2/7/Human/2020/Frankfurt (SARS-CoV-2/FFM7) were isolated and cultivated in Caco2 cells as previously described [17,18]. Virus titers were determined as TCID₅₀/mL in confluent cells in 96-well microtiter plates [19,20].

2.4. Antiviral Assay

Confluent cell cultures were infected with SARS-CoV-2 in 96-well plates at a multiplicity of infection (MOI) of 0.01 in the absence or presence of the drug. The cytopathogenic effect (CPE) was assessed visually 48 h post-infection [19]. Concentrations that inhibited CPE formation by 50% (IC₅₀) were determined using CalcuSyn (Biosoft, Cambridge, UK).

2.5. Viability Assay

Cell viability was determined by 3-(4,5-dimethylthiazol-2-yl)-2,5-diphenyltetrazolium bromide (MTT) assay modified after Mosman [21], as previously described [22]. Confluent cell cultures in 96-well plates were incubated with the drug for 48 h. Then, 25 µL of MTT solution (2 mg/mL (*w/v*) in PBS) were added per well, and the plates were incubated at 37 °C for an additional 4 h. After this, the cells were lysed using 200 µL of a buffer containing 20% (*w/v*) sodium dodecylsulfate and 50% (*v/v*) *N,N*-dimethylformamide with the pH adjusted to 4.7 at 37 °C for 4 h. Absorbance was determined at 570 nm for each well using a 96-well multiscanner (Tecan, Crailsheim, Germany). After subtracting of the background absorption, the results are expressed as percentage viability relative to control cultures that received no drug. Drug concentrations that inhibited cell viability by 50% (CC₅₀) were determined using CalcuSyn (Biosoft).

2.6. Immunostaining for SARS-CoV-2 S Protein

Immunostaining was performed as previously described [23], using a monoclonal antibody directed against SARS-CoV-2 S protein (1:1500 dilution, Sino Biological, Eschborn, Germany) 24 h post-infection.

2.7. Caspase 3/7 Activation

Caspase 3/7 activation was determined using the Caspase-Glo[®] 3/7 Assay (Promega, Walldorf, Germany) according to the manufacturer's instructions.

2.8. qPCR

SARS-CoV-2 RNA from the cell culture supernatant samples was isolated using AVL buffer and the QIAamp Viral RNA Kit (Qiagen, Hilden, Germany) according to the manufacturer's instructions. Absorbance-based quantification of the RNA yield was performed using the Genesys 10S UV-Vis Spectrophotometer (Thermo Fisher Scientific, Dreieich, Germany). RNA was subjected to OneStep qRT-PCR analysis using the Luna Universal One-Step RT-qPCR Kit (New England Biolabs, Frankfurt am Main, Germany) and a CFX96 Real-Time System, C1000 Touch Thermal Cycler (Bio-Rad, Feldkirchen, Germany). Primers were adapted from the WHO protocol²⁹ targeting the open reading frame for RNA-dependent RNA polymerase (RdRp): RdRP_SARSr-F2 (GTG ARA TGG TCA TGT GTG GCG G) and RdRP_SARSr-R1 (CAR ATG TTA AAS ACA CTA TTA GCA TA) using 0.4 µM per reaction. Standard curves were created using plasmid DNA (pEX-A128-RdRP) harboring the corresponding amplicon regions for RdRp target sequence according to GenBank Accession number NC_045512. For each condition, three biological replicates were used. The mean and standard deviation were calculated for each group.

2.9. Western Blot

Cells were lysed using Triton-X-100 sample buffer (Sigma-Aldrich), and proteins were separated by SDS-PAGE. Detection occurred by using specific antibodies against SARS-CoV-2 N (1:1000 dilution, SARS-CoV-2 Nucleocapsid Antibody, Rabbit monoclonal antibody (Mab), #40143-R019, Sino Biological), ACE2 (1:500 dilution, Anti-ACE2 antibody, #ab15348, Abcam, Berlin, Germany), TMPRSS2 (1:1000 dilution, Recombinant Anti-TMPRSS2 antibody [EPR3861], #ab92323, Abcam), and GAPDH (1:1000 dilution, Anti-GAPDH Human Polyclonal Antibody, #2275-PC-100, Trevigen, Wiesbaden, Germany). Protein bands were visualized by laser-induced fluorescence using an infrared scanner for protein quantification (Odyssey, Li-Cor Biosciences, Bad Homburg, Germany).

2.10. Sample Preparation for LC-MS

Preparation of samples was performed as previously described [24] and labeled with TMTpro multiplexing reagents.

2.11. Targeted Analysis by SPS-MS³

Mass spectrometry data were acquired in centroid mode on an Orbitrap Fusion Lumos mass spectrometer hyphenated to an easy-nLC 1200 nano HPLC system using a nanoFlex ion source (ThermoFisher Scientific) applying a spray voltage of 2.6 kV with the transfer tube heated to 300 °C and a funnel RF of 30%. Internal mass calibration was enabled (lock mass 445.12003 *m/z*). Peptides were separated on a self-made, 32 cm long, 75 µm ID fused-silica column, packed in house with 1.9 µm C18 particles (ReproSil-Pur, Dr. Maisch, Ammerbuch-Entringen, Germany) and heated to 50 °C using an integrated column oven (Sonation, Biberach, Germany). The HPLC solvents consisted of 0.1% formic acid in water (Buffer A) and 0.1% formic acid with 80% acetonitrile in water (Buffer B).

Dependent scans were performed on precursors matching a mass list of viral peptides modified with TMTpro reagents and their charge states (mass tolerance was set to 5 ppm for matching precursors). Peptides were eluted by a non-linear gradient from 5% to 40% B over 30 min, followed by a step-wise increase to 95% B in 6 min, which was held for another 9 min. Full scan MS spectra (350–1500 *m/z*) were acquired with a resolution of 120,000 at *m/z* 200, a maximum injection time of 100 ms, and an automatic gain control (AGC) target value of 4×10^5 . The 10 most intense precursors matching the target list per full scan were selected for fragmentation (“Top 10”) and isolated with a quadrupole isolation window of 0.4 Th. MS2 scans were performed in the Orbitrap using a maximum injection time of 300 ms, an AGC target value of 1.5×10^4 , and fragmented using HCD with a normalized collision energy (NCE) of 35% and a fixed first mass of 110 *m/z*. Repeated sequencing of already acquired precursors was limited by setting a dynamic exclusion of 20 s and 10 ppm and advanced peak determination was deactivated.

2.12. Data Analysis

RAW data was processed with Proteome Discoverer 2.4 software. HCD-fragmented spectra were searched against a SARS-CoV-2 proteome FASTA file (UniProt pre-release) by SequestHT and the false discovery rate (FDR) was calculated using a target/decoy-based approach. TMTpro reporter abundances were extracted and used for plotting and statistical analysis.

2.13. Data Availability

The mass spectrometry proteomics data were deposited to the ProteomeXchange Consortium via the PRIDE [25] partner repository with the dataset identifier PXD019950.

3. Results

3.1. The Protease Inhibitor Aprotinin Exerts Superior Anti-SARS-CoV-2 Activity Relative to the Endogenous Protease Inhibitor SERPINA1/alpha-1 Antitrypsin

We compared the anti-SARS-CoV-2 activity of aprotinin [15,26] and SERPINA1/alpha-1 antitrypsin, an endogenous protease inhibitor that is available as a pharmaceutical preparation for the treatment of alpha-1 antitrypsin deficiency [27], against three different SARS-CoV-2 isolates from two lineages (L: SARS-CoV-2/FFM1 and SARS-CoV-2/FFM2; GR: SARS-CoV-2/FFM6) [18]. SARS-CoV-2/FFM1 and SARS-CoV-2/FFM2 were isolated from patients in Hubei province in China, while SARS-CoV/FFM6 was derived from an Italian patient [18].

The aprotinin concentrations that inhibited the formation of cytopathogenic effects (CPEs) by 50% (IC_{50}) in SARS-CoV-2-infected Caco2 cells ranged from 0.81 μ M (SARS-CoV-2/FFM2) to 1.03 μ M (SARS-CoV-2/FFM1) across the three tested SARS-CoV-2 isolates, whereas SERPINA1/alpha-1 antitrypsin did not show significant antiviral effects in the tested concentrations up to 20 μ M (Figure 1A). Similar effects were observed by cell staining for SARS-CoV-2 S protein (Figure 1B and Figure S1, Table 1). Quantification of genomic SARS-CoV-2 RNA using qPCR confirmed that aprotinin inhibits SARS-CoV-2 replication (Figure 1C). Aprotinin (20 μ M) reduced the genomic RNA levels of SARS-CoV-2/FFM1 by 900-fold, those of SARS-CoV-2/FFM2 by 237-fold, and those of SARS-CoV-2/FFM6 by 584-fold.

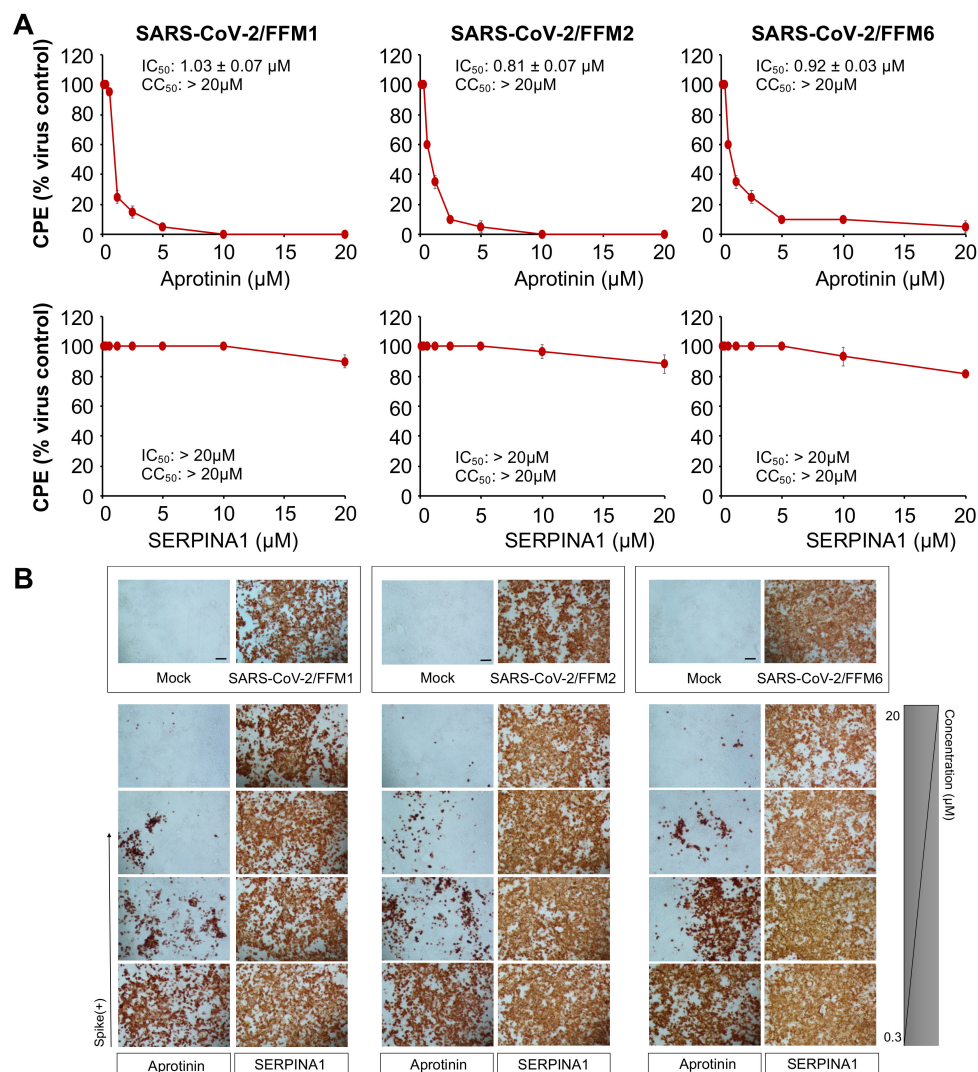


Figure 1. Cont.

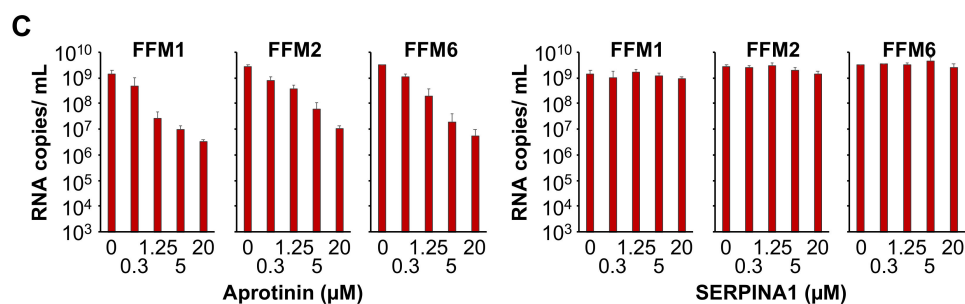


Figure 1. Anti-severe acute respiratory syndrome virus 2 (SARS-CoV-2) effects of aprotinin and SERPINA1/alpha-1 antitrypsin. (A) Concentration-dependent effects of aprotinin and SERPINA1/alpha-1 antitrypsin on SARS-CoV-2-induced cytopathogenic effect (CPE) formation determined 48 h post-infection in Caco2 cells infected at a multiplicity of infection (MOI) of 0.01 with the three different SARS-CoV-2 isolates. The viability of the Caco2 cells was $84.3 \pm 2.7\%$ relative to the untreated control in the presence of 20 μM of aprotinin. (B) Immunostaining for the SARS-CoV-2 S protein in aprotinin- and SERPINA1/alpha-1 antitrypsin-treated Caco2 cells infected at an MOI of 0.01 with the three different SARS-CoV-2 isolates as determined 48 h post-infection. The protease inhibitors were tested at four concentrations in 1:4 dilution steps ranging from 20 to 0.3125 μM . A quantification is provided in Figure S1. (C) Copy numbers of genomic RNA in Caco2 cells infected with different SARS-CoV-2 isolates (MOI of 0.01) in response to treatment with aprotinin or SERPINA1/alpha-1 antitrypsin as determined 48 h post-infection. FFM1, 1/Human/2020/Frankfurt; FFM2, 2/Human/2020/Frankfurt; FFM6, 6/Human/2020/Frankfurt.

Table 1. Aprotinin concentrations that reduce SARS-CoV-2-induced cytopathogenic effect (CPE) formation, SARS-CoV-2 spike (S) levels, and SARS-CoV-2-induced caspase 3/7 activation by 50% (IC_{50}) as determined in Caco2 cells infected with different SARS-CoV-2 isolates (MOI of 0.01) 48 h post-infection.

	IC_{50} (μM)		
	FFM1	FFM2	FFM6
CPE formation	1.03 ± 0.07	0.81 ± 0.07	0.92 ± 0.03
S levels	0.79 ± 0.15	1.04 ± 0.21	1.65 ± 0.30
Caspase 3/7 activation	0.41 ± 0.25	0.32 ± 0.09	0.73 ± 0.40

Both aprotinin and SERPINA1/alpha-1 antitrypsin are trypsin inhibitors [26,28]. To verify the integrity of the used protease inhibitor samples, we tested their capacity to antagonize trypsin and enable Caco2 and A549 cell adhesion. The results confirmed that both protease inhibitors are active (Figure S2). Taken together, these findings indicate differences in the protease inhibitor spectrum of aprotinin and SERPINA1/alpha-1 antitrypsin that result in different effects on SARS-CoV-2 replication.

3.2. Quantification of the Antiviral Effects of Aprotinin by Measuring SARS-CoV-2-Induced Caspase 3/7 Activation

Different viruses, including SARS-CoV-2, have been shown to induce caspase 3 activation [29–32], and virus-induced caspase 3 activation has been used as read-out in assays that quantify the antiviral effects of drug candidates [31]. Hence, we used the Caspase-Glo[®] 3/7 Assay (Promega) as an additional quantitative method to determine the anti-SARS-CoV-2 activity of aprotinin. The results confirmed those obtained by CPE formation and S expression resulting in similar IC_{50} values (Figure 2, Table 1).

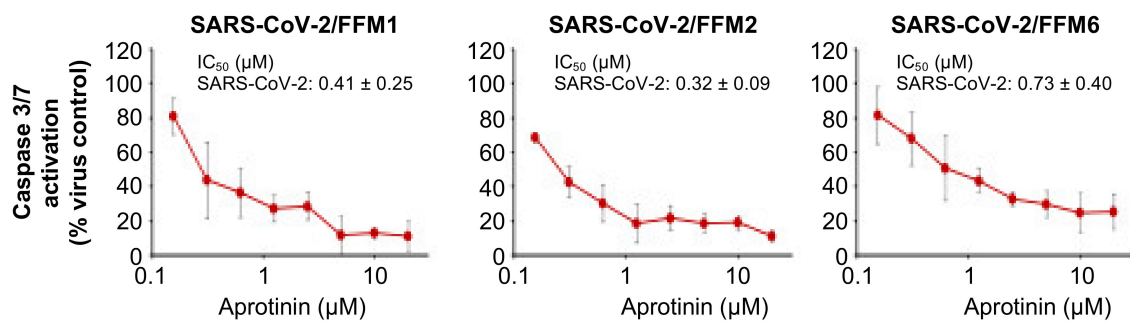


Figure 2. Effects of aprotinin on SARS-CoV-2-induced caspase 3/7 activation. Caspase 3/7 activity was determined in Caco2 cells infected with different SARS-CoV-2 isolates (MOI of 0.01) 48 h post-infection.

3.3. Aprotinin Inhibits Virus Entry

Protease inhibitors were suggested to interfere with SARS-CoV-2 replication predominantly as entry inhibitors that prevent S cleavage and activation [15]. In agreement, aprotinin addition after a one-hour adsorption period did not significantly interfere with SARS-CoV-2 replication in one round of a replication assay, in which virus titers were determined 8 h post-infection with an MOI of 0.1 (Figure 3A). In contrast, remdesivir, which was anticipated to interfere with the replication of the viral genome, inhibited SARS-CoV-2 replication when added post-infection (Figure 3A).

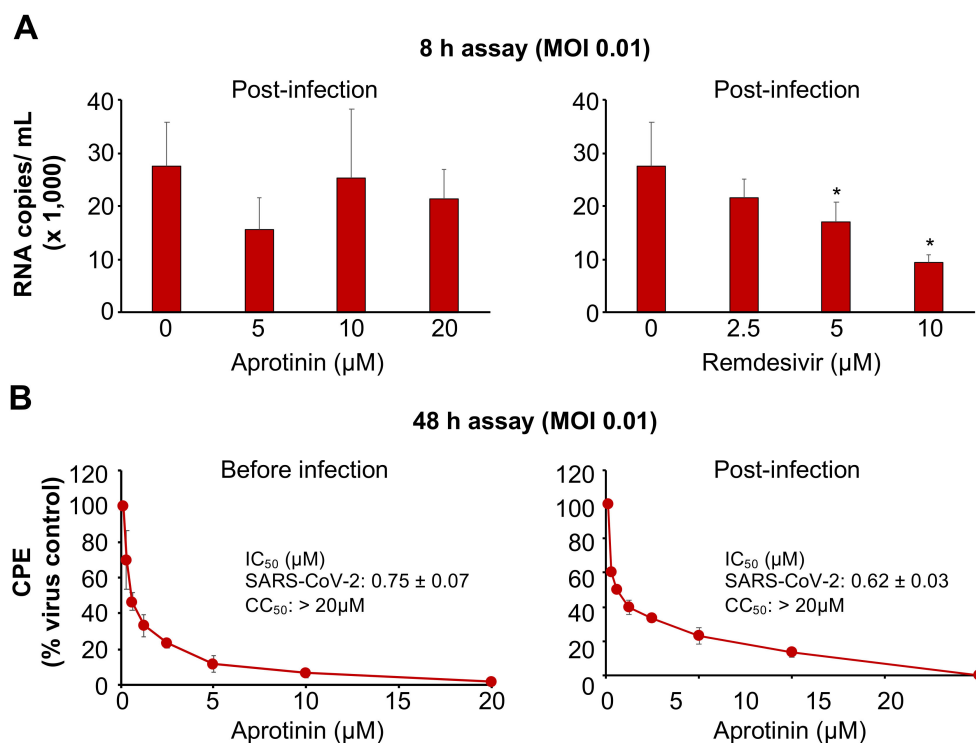


Figure 3. Anti-SARS-CoV-2 effects of aprotinin when administered post-infection. For post-infection experiments, the cells were incubated with the virus for a one-hour adsorption period. Then, the cells were washed three times in PBS prior to the addition of the drug. (A) The effects of aprotinin and the RNA polymerase inhibitor remdesivir (a positive control drug that interferes with virus replication after virus entry) on virus replication as determined by qPCR in SARS-CoV-2/FFM1 (MOI of 0.1)-infected Caco2 cells 8 h post-infection (after approximately one round of replication). * $p < 0.05$ as determined by one-way ANOVA and Dunnett's multiple comparison test. (B) The effects of aprotinin on cytopathogenic effect (CPE) formation in SARS-CoV-2/FFM1 (MOI of 0.01)-infected Caco2 cells were determined 48 h post-infection.

3.4. Aprotinin May Interfere with SARS-CoV-2-Mediated Downregulation of Host Cell Protease Inhibitors

Notably, aprotinin exerted similar anti-SARS-CoV-2 effects when added before or after infection of Caco2 cells with a lower MOI (0.01) in a 48 h assay (Figure 3B). In this format, aprotinin probably inhibits the later rounds of SARS-CoV-2 replication, but other mechanisms may also contribute.

Host cell protease inhibitors interfere with the activity of proteases such as TMPRSS2 [33,34] that mediate SARS-CoV-2 cell entry by cleaving and activating the viral S protein [9,11,12]. An analysis of the effect of SARS-CoV-2 infection on host cell protease inhibitors using proteomics data from SARS-CoV-2-infected Caco2 cells [35] showed that the endogenous protease inhibitors SPINT1 (Kunitz-type protease inhibitor 1), SPINT2 (Kunitz-type protease inhibitor 2), and SERPINA1 (alpha-1-antitrypsin) are present at lower levels in SARS-CoV-2-infected cells than in non-infected control cells 24 h post-infection (Figure 4A). Translatome data from the same dataset [35] indicated that the translation of SERPINA1 and SPINT2 (but not that of SPINT1) is also reduced in SARS-CoV-2-infected cells (Figure 4B). Hence, SARS-CoV-2 infection results in the downregulation of endogenous protease inhibitors, which may support SARS-CoV-2 replication. Thus, compensation for downregulated endogenous protease inhibitors may contribute to the antiviral effects of aprotinin.

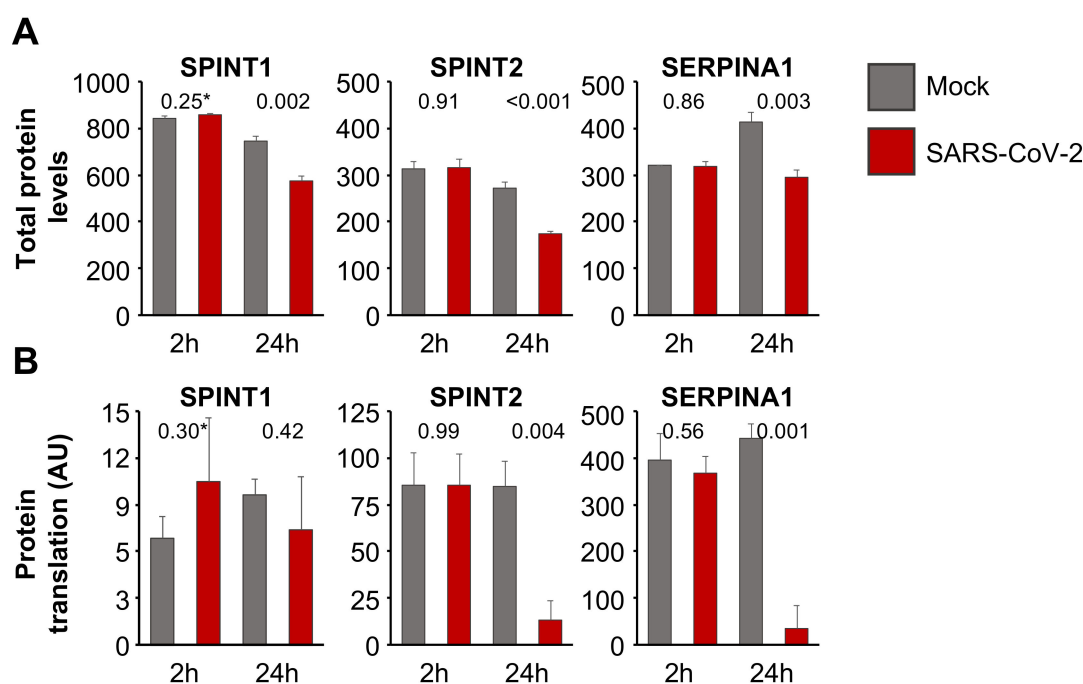


Figure 4. Regulation of host cell protease inhibitors in SARS-CoV-2-infected cells. (A) Total protein levels based on a publicly available proteomics dataset [35], indicating cellular levels of endogenous protease inhibitors in SARS-CoV-2 (MOI of 1)-infected Caco2 cells 2 h and 24 h post-infection. Data were normalized using summed intensity normalization for sample loading, followed by internal reference scaling and trimmed mean of M normalization. * *p*-values as determined using a two-sided Student's *t*-test. (B) Mean protein translation of endogenous protease inhibitors in arbitrary units (AU) (normalized and corrected summed peptide spectrum matches (PSMs) were averaged) in SARS-CoV-2 (MOI of 1)-infected Caco2 cells 2 h and 24 h post-infection based on a publicly available translatome dataset [35]. * *p*-values as determined using a two-sided Student's *t*-test.

3.5. Aprotinin Exerts Anti-SARS-CoV-2 Activity in Air-Liquid Interface (ALI) Cultures from Primary Bronchial Epithelial Cells

We also investigated the effects of aprotinin in SARS-CoV-2-infected air-liquid interface (ALI) cultures from primary bronchial epithelial cells. A targeted proteomics assay demonstrated that aprotinin 20 μ M suppressed the expression of the SARS-CoV-2 proteins N (nucleocapsid protein) and

M (membrane protein) in SARS-CoV-2-infected ALI cultures (Figure 5A, Table S1). The results for N were confirmed by Western blots in the ALI cultures infected with SARS-CoV-2/FFM7 (Figure 5B). SARS-CoV-2/FFM7 (G lineage) is an alternative isolate derived from a patient from Israel [18]. Aprotinin also suppressed SARS-CoV-2 S expression in SARS-CoV-2/FFM7-infected Calu-3 lung adenocarcinoma cells (Figure S3).

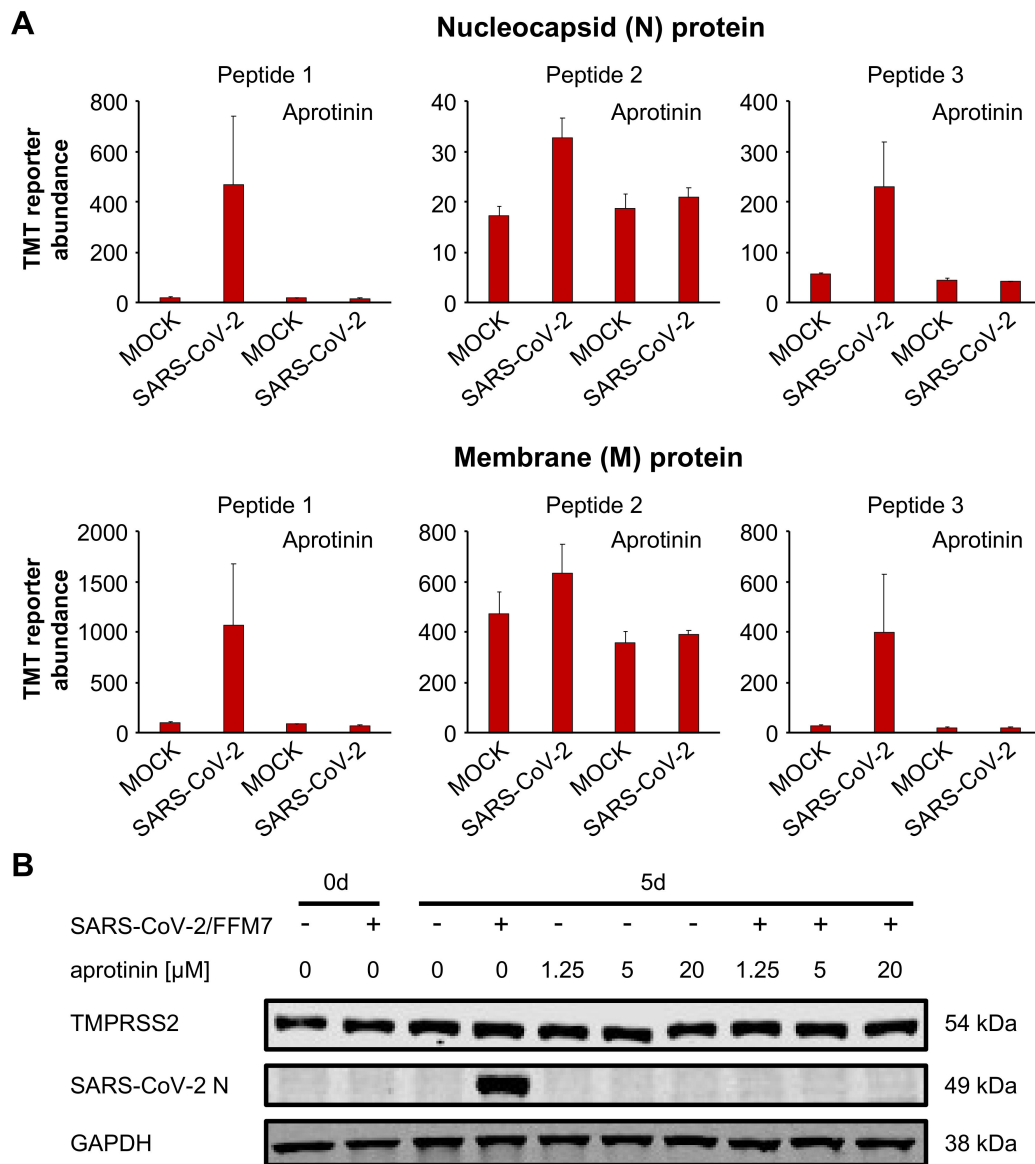


Figure 5. Antiviral effects of aprotinin in SARS-CoV-2-infected air–liquid interface (ALI) cultures from primary bronchial epithelial cells. **(A)** Abundance of the SARS-CoV-2 proteins N (nucleocapsid) and M (membrane) in primary bronchial epithelial cell ALI cultures infected with SARS-CoV-2/FFM1 (MOI of 1) in the presence or absence of aprotinin (20 μ M) as determined 5 days post-infection by multiplexed mass spectrometry analysis using acquisition targeting of previously identified viral peptides modified with TMTpro. The detailed data are presented in Table S1. **(B)** Western blots indicating cellular SARS-CoV-2 N and TMPRSS2 levels in primary bronchial epithelial cell ALI cultures infected with SARS-CoV-2/7/Human/2020/Frankfurt (FFM7) (MOI of 1) in the presence or absence of aprotinin as detected 5 days post infection. GAPDH was served as the loading control. Uncropped Western blots are shown in Figure S4.

4. Discussion

Herein, we showed that aprotinin inhibits SARS-CoV-2 replication predominantly as an entry inhibitor, probably via interfering with SARS-CoV-2 S activation by TMPRSS2. Notably, SERPINA1/alpha-1 antitrypsin, which is available as a pharmaceutical preparation for the treatment of alpha-1 antitrypsin deficiency [27], did not inhibit SARS-CoV-2 replication in the same concentration range. Further investigations will have to elucidate the differences between aprotinin and SERPINA1/alpha-1 antitrypsin that are responsible for the discrepancy in anti-SARS-CoV-2 activity. Notably, SERPINA1/alpha-1 antitrypsin was shown to inhibit TMPRSS2 in an enzymatic assay and is suggested as an antiviral treatment for COVID-19 [36]. A clinical trial testing SERPINA1/alpha-1 antitrypsin for the treatment of COVID-19 has recently been started (ClinicalTrials.gov Identifier: NCT04385836). Based on our data, however, SERPINA1/alpha-1 antitrypsin is not expected to exert direct antiviral effects in COVID-19 patients. Our findings also indicate that antiviral therapy candidates should be tested for their effects on complete replication-competent viruses in permissive cells.

Aprotinin exerted anti-SARS-CoV-2 effects in three cell culture models (Caco2, Calu-3, and air–liquid interface cultures from primary bronchial epithelial cells) and against three SARS-CoV-2 strains (FFM1, FFM2, FFM6, and FFM7). Notably, another study became available during the revision of our manuscript that detected anti-SARS-CoV-2 activity of aprotinin in Calu-3 cells [37]. Our findings are also in agreement with studies that reported other TMPRSS2 inhibitors to inhibit SARS-CoV-2 entry and replication [11–13]. In addition, furin has been shown to cleave and activate SARS-CoV-2 S and furin inhibitors have been demonstrated to exert anti-SARS-CoV-2 effects [38].

Endogenous protease inhibitors may interfere with the activation of virus surface proteins such as S by host cell proteases [9,11,12,33,34]. Our analysis of proteomics and transcriptome data from SARS-CoV-2-infected Caco2 cells [35] revealed a downregulation of endogenous protease inhibitors in response to SARS-CoV-2 infection, which may contribute to efficient SARS-CoV-2 replication. In addition to entry inhibition, compensation for downregulated endogenous proteases may, hence, further contribute to the antiviral activity of aprotinin during later rounds of SARS-CoV-2 replication.

The clinical potency of aprotinin is typically measured in kallikrein inhibitor units (KIUs) [14,39]. Therapeutic aprotinin plasma levels were described to reach 147 ± 61 KIU/mL after the administration of 1,000,000 KIU [39]. Moreover, an aerosol preparation of aprotinin, which is likely to result in increased local aprotinin concentrations in the lung, is approved for the treatment of influenza in Russia [14]. The aprotinin IC_{50} values for SARS-CoV-2-induced CPE formation, S expression, and apoptosis induction ranged from 0.32 to 1.65 μ M, which is equivalent to 4.0 KIU and 20.6 KIU, respectively. Hence, aprotinin interferes with SARS-CoV-2 infection in therapeutically achievable concentrations.

Aprotinin exerts pro- and antithrombotic effects by balancing fibrinolysis and thrombus formation and is approved for the prevention of blood loss during surgery. It interferes with the fibrinolysis of established thrombi by plasmin, but also inhibits contact-activated thrombus formation in the blood stream [26,40–43]. Late-stage, severe COVID-19 disease has been associated with disseminated intravascular coagulation and thrombosis (COVID-19-related coagulopathy) [44]. Based on the available data, it is not clear whether aprotinin may exert pro- or antithrombotic effects in patients suffering from COVID-19-related coagulopathy. Thus, aprotinin would have to be considered with care for such patients.

However, antiviral treatment may anyway be of limited impact in late-stage COVID-19 disease, during which, damage is anticipated to be largely caused by immunopathology and not by virus replication [42,45,46]. Hence, the main potential of antiviral drugs may lie in the early treatment of COVID-19 patients to suppress virus replication and, through this, to prevent COVID-19 progression into a severe, life-threatening disease. Local aprotinin therapy of the airways and the lungs using an aerosol, which is clinically approved in Russia and has been reported to be very well tolerated in influenza patients [14], may have particular potential as such an antiviral treatment for early stage COVID-19 disease. Notably, aprotinin may additionally prevent the very early stages of lung injury by

inhibition of matrix metalloproteinases and, in turn, of the cytokine storm that eventually results in severe, systemic COVID-19 disease [26].

5. Conclusions

In conclusion, therapeutic aprotinin concentrations inhibit SARS-CoV-2 replication as entry inhibitors and by compensating for downregulated cellular protease inhibitors during later replication cycles. Local treatment of the respiratory tract using an aprotinin aerosol, which is approved in Russia for the treatment of influenza [14], may be a particularly promising strategy to suppress virus replication and lung injury early and to prevent COVID-19 progression into a severe, systemic disease.

Supplementary Materials: The following are available online at <http://www.mdpi.com/2073-4409/9/11/2377/s1>, Figure S1: Quantification of immunostaining of SARS-CoV-2-infected Caco2 cells with and without treatment of aprotinin or SERPINA1/alpha-1 antitrypsin; Figure S2: Trypsin inhibition by aprotinin and SERPINA1/alpha-1 antitrypsin; Figure S3: Quantification of immunostaining for the spike protein in SARS-CoV-2-infected Calu-3 cells; Figure S4: Uncropped Western blots; Table S1: Detailed mass spectrometry data.

Author Contributions: Conceptualization, M.N.W., M.M. and J.C.J.; methodology, C.B., G.R., D.J., P.B., C.M., M.N.W., M.M. and J.C.J.; formal analysis, all authors; investigation, D.B., M.B., K.L., J.E.M., K.K. and J.C.J.; resources, S.C., C.M., M.N.W., M.M. and J.C.J.; data curation, D.B., M.B., K.-M.M., J.E.M., K.K., C.M., M.N.W., M.M. and J.C.J.; writing—original draft preparation, M.M.; writing—review and editing, all authors; supervision, C.M., M.N.W., M.M. and J.C.J.; project administration, M.M. and J.C.J.; funding acquisition, J.C.J. All authors have read and agreed to the published version of the manuscript.

Funding: This research was funded by the Hilfe für krebserkrankte Kinder Frankfurt e.V. and the Frankfurter Stiftung für krebserkrankte Kinder. The APC was funded by Goethe University.

Conflicts of Interest: The authors declare no conflicts of interest. The funders had no role in the design of the study; in the collection, analyses, or interpretation of data; in the writing of the manuscript, or in the decision to publish the results.

References

- Chen, N.; Zhou, M.; Dong, X.; Qu, J.; Gong, F.; Han, Y.; Qiu, Y.; Wang, J.; Liu, Y.; Wei, Y.; et al. Epidemiological and clinical characteristics of 99 cases of 2019 novel coronavirus pneumonia in Wuhan, China: A descriptive study. *Lancet* **2020**, *395*, 507–513. [[CrossRef](#)]
- Coronaviridae Study Group of the International Committee on Taxonomy of Viruses. The species Severe acute respiratory syndrome-related coronavirus: Classifying 2019-nCoV and naming it SARS-CoV-2. *Nat. Microbiol.* **2020**, *5*, 536–544. [[CrossRef](#)]
- Dong, E.; Du, H.; Gardner, L. An interactive web-based dashboard to track COVID-19 in real time. *Lancet Infect. Dis.* **2020**, *20*, 533–534. [[CrossRef](#)]
- Lu, R.; Zhao, X.; Li, J.; Niu, P.; Yang, B.; Wu, H.; Wang, W.; Song, H.; Huang, B.; Zhu, N.; et al. Genomic characterisation and epidemiology of 2019 novel coronavirus: Implications for virus origins and receptor binding. *Lancet* **2020**, *395*, 565–574. [[CrossRef](#)]
- Wu, F.; Zhao, S.; Yu, B.; Chen, Y.M.; Wang, W.; Song, Z.G.; Hu, Y.; Tao, Z.W.; Tian, J.H.; Pei, Y.Y.; et al. A new coronavirus associated with human respiratory disease in China. *Nature* **2020**, *579*, 265–269. [[CrossRef](#)] [[PubMed](#)]
- Zhou, P.; Yang, X.L.; Wang, X.G.; Hu, B.; Zhang, L.; Zhang, W.; Si, H.R.; Zhu, Y.; Li, B.; Huang, C.L.; et al. A pneumonia outbreak associated with a new coronavirus of probable bat origin. *Nature* **2020**, *579*, 270–273. [[CrossRef](#)]
- Zhu, N.; Zhang, D.; Wang, W.; Li, X.; Yang, B.; Song, J.; Zhao, X.; Huang, B.; Shi, W.; Lu, R.; et al. China Novel Coronavirus Investigating and Research Team. *N. Engl. J. Med.* **2020**, *382*, 727–733. [[CrossRef](#)] [[PubMed](#)]
- Cui, J.; Li, F.; Shi, Z.L. Origin and evolution of pathogenic coronaviruses. *Nat. Rev. Microbiol.* **2019**, *17*, 181–192. [[CrossRef](#)]
- Hoffmann, M.; Kleine-Weber, H.; Schroeder, S.; Krüger, N.; Herrler, T.; Erichsen, S.; Schiergens, T.S.; Herrler, G.; Wu, N.H.; Nitsche, A.; et al. SARS-CoV-2 Cell Entry Depends on ACE2 and TMPRSS2 and Is Blocked by a Clinically Proven Protease Inhibitor. *Cell* **2020**, *181*, 271–280.e8. [[CrossRef](#)]

10. Matsuyama, S.; Nao, N.; Shirato, K.; Kawase, M.; Saito, S.; Takayama, I.; Nagata, N.; Sekizuka, T.; Katoh, H.; Kato, F.; et al. Enhanced isolation of SARS-CoV-2 by TMPRSS2-expressing cells. *Proc. Natl. Acad. Sci. USA* **2020**, *117*, 7001–7003. [[CrossRef](#)]
11. Hoffmann, M.; Schroeder, S.; Kleine-Weber, H.; Müller, M.A.; Drosten, C.; Pöhlmann, S. Nafamostat mesylate blocks activation of SARS-CoV-2: New treatment option for COVID-19. *Antimicrob. Agents Chemother.* **2020**, *64*, e00754-20. [[CrossRef](#)] [[PubMed](#)]
12. Yamamoto, M.; Kiso, M.; Sakai-Tagawa, Y.; Iwatsuki-Horimoto, K.; Imai, M.; Takeda, M.; Kinoshita, N.; Ohmagari, N.; Gohda, J.; Semba, K.; et al. The Anticoagulant Nafamostat Potently Inhibits SARS-CoV-2 S Protein-Mediated Fusion in a Cell Fusion Assay System and Viral Infection In Vitro in a Cell-Type-Dependent Manner. *Viruses* **2020**, *12*, 629. [[CrossRef](#)] [[PubMed](#)]
13. Choudhary, S.; Silakari, O. Scaffold morphing of arbidol (umifenovir) in search of multi-targeting therapy halting the interaction of SARS-CoV-2 with ACE2 and other proteases involved in COVID-19. *Virus. Res.* **2020**, *289*, 198146. [[CrossRef](#)] [[PubMed](#)]
14. Zhirnov, O.P.; Klenk, H.D.; Wright, P.F. Aprotinin and similar protease inhibitors as drugs against influenza. *Antiviral Res.* **2011**, *92*, 27–36. [[CrossRef](#)]
15. Shen, L.W.; Mao, H.J.; Wu, Y.L.; Tanaka, Y.; Zhang, W. TMPRSS2: A potential target for treatment of influenza virus and coronavirus infections. *Biochimie* **2017**, *142*, 1–10. [[CrossRef](#)]
16. Van Wetering, S.; van der Linden, A.C.; van Sterkenburg, M.A.; de Boer, W.I.; Kuijpers, A.L.; Schalkwijk, J.; Hiemstra, P.S. Regulation of SLPI and elafin release from bronchial epithelial cells by neutrophil defensins. *Am. J. Physiol. Lung Cell. Mol. Physiol.* **2000**, *278*, L51–L58. [[CrossRef](#)]
17. Hoehl, S.; Berger, A.; Kortenbusch, M.; Cinatl, J.; Bojkova, D.; Rabenau, H.; Behrens, P.; Böddinghaus, B.; Götsch, U.; Naujoks, F.; et al. Evidence of SARS-CoV-2 Infection in Returning Travelers from Wuhan, China. *N. Engl. J. Med.* **2020**, *382*, 1278–1280. [[CrossRef](#)]
18. Toptan, T.; Hoehl, S.; Westhaus, S.; Bojkova, D.; Berger, A.; Rotter, B.; Hoffmeier, K.; Cinatl, J., Jr.; Ciesek, S.; Widera, M. Optimized qRT-PCR Approach for the Detection of Intra- and Extra-Cellular SARS-CoV-2 RNAs. *Int. J. Mol. Sci.* **2020**, *21*, 4396. [[CrossRef](#)]
19. Cinatl, J.; Morgenstern, B.; Bauer, G.; Chandra, P.; Rabenau, H.; Doerr, H.W. Glycyrrhizin, an active component of liquorice roots, and replication of SARS-associated coronavirus. *Lancet* **2003**, *361*, 2045–2046. [[CrossRef](#)]
20. Cinatl, J., Jr.; Michaelis, M.; Morgenstern, B.; Doerr, H.W. High-dose hydrocortisone reduces expression of the pro-inflammatory chemokines CXCL8 and CXCL10 in SARS coronavirus-infected intestinal cells. *Int. J. Mol. Med.* **2005**, *15*, 323–327. [[CrossRef](#)]
21. Mosmann, T. Rapid colorimetric assay for cellular growth and survival: Application to proliferation and cytotoxicity assays. *J. Immunol. Methods.* **1983**, *65*, 55–63. [[CrossRef](#)]
22. Onafuye, H.; Pieper, S.; Mulac, D.; Cinatl, J., Jr.; Wass, M.N.; Langer, K.; Michaelis, M. Doxorubicin-loaded human serum albumin nanoparticles overcome transporter-mediated drug resistance in drug-adapted cancer cells. *Beilstein J. Nanotechnol.* **2019**, *10*, 1707–1715. [[CrossRef](#)] [[PubMed](#)]
23. Cinatl, J.; Cinatl, J.; Weber, B.; Rabenau, H.; Gumbel, H.O.; Chenot, J.F.; Scholz, M.; Encke, A.; Doerr, H.W. In vitro inhibition of human cytomegalovirus replication in human foreskin fibroblasts and endothelial cells by ascorbic acid 2-phosphate. *Antiviral Res.* **1995**, *27*, 405–418. [[CrossRef](#)]
24. Klann, K.; Tascher, G.; Münch, C. Functional Translatome Proteomics Reveal Converging and Dose-Dependent Regulation by mTORC1 and eIF2 α . *Mol. Cell.* **2020**, *77*, 913–925.e4. [[CrossRef](#)] [[PubMed](#)]
25. Perez-Riverol, Y.; Csordas, A.; Bai, J.; Bernal-Llinares, M.; Hewapathirana, S.; Kundu, D.J.; Inuganti, A.; Griss, J.; Mayer, G.; Eisenacher, M.; et al. The PRIDE database and related tools and resources in 2019: Improving support for quantification data. *Nucleic Acids Res.* **2019**, *47*, D442–D450. [[CrossRef](#)] [[PubMed](#)]
26. Solun, B.; Shoefeld, Y. Inhibition of metalloproteinases in therapy for severe lung injury due to COVID-19. *Med. Drug Discov.* **2020**, *7*, 100052. [[CrossRef](#)]
27. Strnad, P.; McElvaney, N.G.; Lomas, D.A. Alpha(1)-Antitrypsin Deficiency. *N. Engl. J. Med.* **2020**, *382*, 1443–1455. [[CrossRef](#)]
28. Gettins, P.G. Serpin structure, mechanism, and function. *Chem. Rev.* **2002**, *102*, 4751–4804. [[CrossRef](#)]
29. Michaelis, M.; Kleinschmidt, M.C.; Doerr, H.W.; Cinatl, J., Jr. Minocycline inhibits West Nile virus replication and apoptosis in human neuronal cells. *J. Antimicrob. Chemother.* **2007**, *60*, 981–986. [[CrossRef](#)]
30. Ren, Y.; Shu, T.; Wu, D.; Mu, J.; Wang, C.; Huang, M.; Han, Y.; Zhang, X.Y.; Zhou, W.; Qiu, Y.; et al. The ORF3a protein of SARS-CoV-2 induces apoptosis in cells. *Cell. Mol. Immunol.* **2020**, *17*, 881–883. [[CrossRef](#)]

31. Xu, M.; Lee, E.M.; Wen, Z.; Cheng, Y.; Huang, W.K.; Qian, X.; Tcw, J.; Kouznetsova, J.; Ogden, S.C.; Hammack, C.; et al. Identification of small-molecule inhibitors of Zika virus infection and induced neural cell death via a drug repurposing screen. *Nat. Med.* **2016**, *22*, 1101–1107. [[CrossRef](#)]
32. Li, S.; Zhang, Y.; Guan, Z.; Li, H.; Ye, M.; Chen, X.; Shen, J.; Zhou, Y.; Shi, Z.L.; Zhou, P.; et al. SARS-CoV-2 triggers inflammatory responses and cell death through caspase-8 activation. *Signal. Transduct. Target. Ther.* **2020**, *5*, 235. [[CrossRef](#)]
33. Esumi, M.; Ishibashi, M.; Yamaguchi, H.; Nakajima, S.; Tai, Y.; Kikuta, S.; Sugitani, M.; Takayama, T.; Tahara, M.; Takeda, M.; et al. Transmembrane serine protease TMPRSS2 activates hepatitis C virus infection. *Hepatology* **2015**, *61*, 437–446. [[CrossRef](#)]
34. Straus, M.R.; Kinder, J.T.; Segall, M.; Dutch, R.E.; Whittaker, G.R. SPINT2 inhibits proteases involved in activation of both influenza viruses and metapneumoviruses. *Virology* **2020**, *543*, 43–53. [[CrossRef](#)]
35. Bojkova, D.; Klann, K.; Koch, B.; Wiedera, M.; Krause, D.; Ciesek, S.; Cinatl, J.; Münch, C. Proteomics of SARS-CoV-2-infected host cells reveals therapy targets. *Nature* **2020**, *583*, 469–472. [[CrossRef](#)]
36. Azouz, N.P.; Klingler, A.M.; Rothenberg, M.E. Alpha 1 Antitrypsin is an Inhibitor of the SARS-CoV2-Priming Protease TMPRSS2. *bioRxiv* **2020**. preprint. [[CrossRef](#)]
37. Bestle, D.; Heindl, M.R.; Limburg, H.; Van Lam van, T.; Pilgram, O.; Moulton, H.; Stein, D.A.; Hards, K.; Eickmann, M.; Dolnik, O.; et al. TMPRSS2 and furin are both essential for proteolytic activation of SARS-CoV-2 in human airway cells. *Life Sci. Alliance* **2020**, *3*, e202000786. [[CrossRef](#)]
38. Cheng, Y.W.; Chao, T.L.; Li, C.L.; Chiu, M.F.; Kao, H.C.; Wang, S.H.; Pang, Y.H.; Lin, C.H.; Tsai, Y.M.; Lee, W.H.; et al. Furin Inhibitors Block SARS-CoV-2 Spike Protein Cleavage to Suppress Virus Production and Cytopathic Effects. *Cell Rep.* **2020**, *33*, 108254. [[CrossRef](#)]
39. Levy, J.H.; Bailey, J.M.; Salmenperä, M. Pharmacokinetics of aprotinin in preoperative cardiac surgical patients. *Anesthesiology* **1994**, *80*, 1013–1018. [[CrossRef](#)]
40. Dietrich, W. Reducing thrombin formation during cardiopulmonary bypass: Is there a benefit of the additional anticoagulant action of aprotinin? *J. Cardiovasc. Pharmacol.* **1996**, *27*, S50–S57. [[CrossRef](#)]
41. Terrell, M.R.; Walenga, J.M.; Koza, M.J.; Pifarré, R. Efficacy of aprotinin with various anticoagulant agents in cardiopulmonary bypass. *Ann. Thorac. Surg.* **1996**, *62*, 506–511. [[CrossRef](#)]
42. Kuitunen, A.; Hiippala, S.; Vahtera, E.; Rasi, V.; Salmenperä, M. The effects of aprotinin and tranexamic acid on thrombin generation and fibrinolytic response after cardiac surgery. *Acta Anaesthesiol. Scand.* **2005**, *49*, 1272–1279. [[CrossRef](#)] [[PubMed](#)]
43. Sperzel, M.; Huetter, J. Evaluation of aprotinin and tranexamic acid in different in vitro and in vivo models of fibrinolysis, coagulation and thrombus formation. *J. Thromb. Haemost.* **2007**, *5*, 2113–2118. [[CrossRef](#)]
44. Marchandot, B.; Sattler, L.; Jesel, L.; Matsushita, K.; Schini-Kerth, V.; Grunebaum, L.; Morel, O. COVID-19 Related Coagulopathy: A Distinct Entity? *J. Clin. Med.* **2020**, *9*, 1651. [[CrossRef](#)]
45. Lega, S.; Naviglio, S.; Volpi, S.; Tommasini, A. Recent Insight into SARS-CoV2 Immunopathology and Rationale for Potential Treatment and Preventive Strategies in COVID-19. *Vaccines* **2020**, *8*, 224. [[CrossRef](#)] [[PubMed](#)]
46. Polycarpou, A.; Howard, M.; Farrar, C.A.; Greenlaw, R.; Fanelli, G.; Wallis, R.; Klavinskis, L.S.; Sacks, S. Rationale for targeting Complement in COVID-19. *EMBO Mol. Med.* **2020**, *12*, e202012642.

Publisher's Note: MDPI stays neutral with regard to jurisdictional claims in published maps and institutional affiliations.



© 2020 by the authors. Licensee MDPI, Basel, Switzerland. This article is an open access article distributed under the terms and conditions of the Creative Commons Attribution (CC BY) license (<http://creativecommons.org/licenses/by/4.0/>).